



Impact of climate change on river flooding assessed with different spatial model resolutions

M.J. Booij*

Department of Water Engineering and Management, University of Twente, P.O. Box 217, 7500 AE Enschede, The Netherlands

Received 26 April 2002; revised 9 July 2004; accepted 30 July 2004

Abstract

The impact of climate change on flooding in the river Meuse is assessed on a daily basis using spatially and temporally changed climate patterns and a hydrological model with three different spatial resolutions. This is achieved by selecting a hydrological modelling framework and implementing appropriate model components, derived in an earlier study, into the selected framework (HBV). Additionally, two other spatial resolutions for the hydrological model are used to evaluate the sensitivity of the model results to spatial model resolution and to allow for a test of the model appropriateness procedure. Generations of a stochastic precipitation model under current and changed climate conditions have been used to assess the climate change impacts. The average and extreme discharge behaviour at the basin outlet is well reproduced by the three versions of the hydrological model in the calibration and validation, the results become somewhat better with increasing model resolution. The model results with synthetic precipitation under current climate conditions show a small overestimation of average discharge behaviour and a considerable underestimation of extreme discharge behaviour. The underestimation of extreme discharges is caused by the small-scale character of the observed precipitation input at the sub-basin scale. The general trend with climate change is a small decrease of the average discharge and a small increase of discharge variability and extreme discharges. The variability in extreme discharges for climate change conditions increases with respect to the simulations for current climate conditions. This variability results both from the stochasticity of the precipitation process and the differences between the climate models. The total uncertainty in river flooding with climate change (over 40%) is much larger than the change with respect to current climate conditions (less than 10%). However, climate changes are systematic changes rather than random changes and thus the large uncertainty range will be shifted to another level corresponding to the changed average situation.

© 2004 Elsevier B.V. All rights reserved.

Keywords: Climate changes; River flooding; Model resolution; Spatial scale; Appropriateness; HBV model; Meuse basin

1. Introduction

Global climate changes induced by increases in greenhouse gas concentrations is likely to increase temperatures, change precipitation patterns and

* Fax: +31 53 489 5377.

E-mail address: m.j.booij@ctw.utwente.nl.

probably raise the frequency of extreme events (IPCC, 2001). These changes may have serious impacts on society, e.g. on river deltas because of both sea level rise and an increased occurrence of flooding events (Jacobs et al., 2000). Flooding events may cause enormous economical, social and environmental damage and even loss of lives. This necessitates the application of robust and accurate flood estimation procedures to provide a strong basis for investments in flood protection measures with climate change.

Flood estimation with climate change cannot be done on a purely statistical basis, because extreme value distributions may change in future. Therefore, a more physically based approach should be used, which incorporates meteorological and hydrological information. This approach can be carried out with analytical methods or with Monte Carlo simulation. The first method uses simple, analytically solvable equations, for example intensity–duration–frequency (IDF) curves (e.g. Blöschl and Sivapalan, 1997) in the meteorological part and derived flood frequency distributions in the hydrological part (e.g. Goel et al., 2000). The second method involves the generation of synthetic meteorological time series (e.g. Wilks, 1998) as input to a rainfall–runoff model (e.g. Lamb, 1999) to derive discharge series. An extreme value distribution function can then be fitted to the peak discharges as in the statistical approach. Diermanse (2001) has identified two drawbacks when applying analytical methods, i.e. the spatial heterogeneity of inputs and processes is not incorporated, and the interaction of different flood generating mechanisms is not contained in these methods. One of the reasons is that equations cannot be too complex, because they should be solved analytically. The Monte Carlo approach does not have this requirement and can be used in climate change situations. Moreover, with the latter approach an uncertainty assessment can be done to evaluate the validity of the estimated floods with climate change.

To use the physically based flood frequency analysis, a selection of a meteorological model (i.e. a precipitation model) and a river basin model should be made. The choice of the meteorological model is described extensively by Booij (2002a), where a stochastic model was found to be appropriate for generating precipitation with climate change for the Meuse river basin (surface area about 20,000 km²) in

Western Europe. The results of this study and the input of other climatological variables will be briefly discussed here. The emphasis in this study is on the selection of a river basin model.

A broad palette of models is available ranging from simple, lumped black-box models to complex, distributed models including lots of physics and mathematics. These include empirical models, conceptual models and physically based models. These divisions are somewhat arbitrary and hybrid forms exist in which different methods are combined. The complexity of models does not only depend on the model class to which they belong, but also on the processes incorporated, the process formulations used and the different space and time scales employed. In general, models should be sufficiently detailed to capture the dominant processes and natural variability, but not unnecessarily refined that computation time is wasted or data availability is limited. It would seem that an optimum model complexity associated with minimum total uncertainty exists, with a balance in uncertainties from input, model structure and parameters. This raises the question what such an appropriate model should look like given the specific modelling objective and research area. More specifically, which physical processes and data should be incorporated and which mathematical process formulations should be used and at which spatial and temporal scale, to obtain an appropriate model level.

Booij (2003) has developed a model appropriateness procedure, in which subsequently dominant processes, appropriate scales and associated appropriate process formulations are determined. The emphasis has been put on the determination of the appropriate spatial scales. The appropriate model components derived in that study are implemented here into an existing modelling framework to obtain the appropriate model. Two other spatial resolutions for the hydrological model are constructed to assess the sensitivity of the results to spatial model resolution. Previous studies (Middelkoop and Parmet, 1998; Gellens and Roulin, 1998) have suggested that climate change will result in an increase of flood frequencies for the Meuse basin. However, they did not attempt to simulate discharge behaviour on a daily basis using spatially and temporally changed climate patterns.

The objective of this paper is to assess the impact of climate change on flooding in the river Meuse on

a daily basis using spatially and temporally changed climate patterns and the three constructed hydrological models. This objective is achieved by selecting a hydrological modelling framework and implementing the appropriate model components into this framework (Section 2). The observed and modelled climatological and hydrological data are briefly described in Section 3. The estimation of the model parameters and the model experiments are considered in Section 4 and in Section 5 the results are presented and discussed. Finally, the conclusions are drawn in Section 6.

2. Selection and description of river basin model

The appropriate model components for the current research objective have been derived by Booij (2002a). The most important processes in the context of climate change impacts on river flooding were found to be precipitation, evapotranspiration, infiltration excess overland flow, saturation excess overland flow, subsurface storm flow, subsurface flow and river flow. The appropriate spatial model scale has been assessed at about 10 km with a corresponding temporal scale of 1 day (Booij, 2003). This appropriate model scale consists of several individual variable scales, e.g. for land use (about 5 km) and for extreme daily precipitation (about 20 km, see Booij, 2002b). Surface flow can be appropriately modelled with diffusion or kinematic wave-based methods, whereas subsurface flow at a 10–60 km scale can be simulated using simplified equations such as Green–Ampt. Potential evapotranspiration should be preferably calculated using the Penman–Monteith equation or the Priestley–Taylor formulation if not all the data are available.

This brief summary of the components of an appropriate model already gives some directives about which kind of model can be used for implementation of these appropriate components. Three main categories of hydrological models have been considered in the introduction. Empirical models are based on mathematical equations which do not take into account the underlying physical processes and therefore are not useful for implementation of the appropriate model components. Physically based models like SHE (Abbott et al., 1986) and IHDM

(Beven et al., 1987), on the other hand, incorporate physical laws based on the conservation of mass, momentum and energy. The governing equations include a lot of parameters and must be solved numerically. The high amount of parameters may result in different parameter combinations giving equally good output performances, which is usually labelled as overparameterisation. The main solution is to use more data, either through direct measurements of parameters in the field or through measurement of intern state variables like soil moisture contents. Besides this overparameterisation effect, physically based models generally incorporate too many processes and too complex formulations at a too detailed scale in the context of climate change and river flooding as revealed by the appropriate components found. Therefore, the so-called conceptual models seem to be an attractive alternative, although they still suffer from the overparameterisation problem. Examples are given by Beven (1993) and Uhlenbrook et al. (1999), who got very good model performances for different parameter sets. Conceptual models are usually able to capture the dominating hydrological processes at the appropriate scale with accompanying formulations. The conceptual models can therefore be considered as a nice compromise between the need for simplicity on the one hand and the need for a firm physical basis on the other hand. A disadvantage may be that it is generally impossible to derive the model parameters directly from field measurements and therefore calibration techniques must be used (Refsgaard, 1996). Well-known conceptual models are the Stanford watershed model (Crawford and Linsley, 1966), the HBV model (Bergström and Forsman, 1973) and the Precipitation Runoff Modelling System—PRMS (Leavesley et al., 1983).

The next step is to choose one of the available conceptual models for the implementation of the appropriate model concepts. Therefore, conceptual model intercomparisons may be used like the ones performed by Franchini and Pacciani (1991) for seven models and Ye et al. (1997) for three models. However, these intercomparisons do not encompass all important conceptual models and therefore the model intercomparison of Passchier (1996) has been used as primary directive for the choice of a model. He selected 5 ‘event’ (single runoff event) models and 10 continuous hydrological models out of 31 models

for comparison on the basis of 7 criteria (e.g. state of the art, application areas, level of complexity and detail). His research objective was to select models for rainfall–runoff modelling of the Rhine and Meuse basin with emphasis on four specific aims, namely land use impact modelling, climate change impact modelling, real-time flood forecasting and physically based flood frequency analysis. Besides these four aims, 10 evaluation criteria (e.g. reliability, scientific basis, scale, availability) have been used for all of the 31 models. Four continuous models [PRMS, SACRAMENTO (Burnash, 1995), HBV and SWMM (Huber, 1995)] and one event model (HEC-1; Feldman, 1995) were evaluated as the best ones. These results and the results for the four specific research aims were used to select a few appropriate models for each of the four research aims. The HEC-1 and HBV models were found to be most appropriate for flood frequency analysis, the HBV and SLURP (Kite, 1995) models for assessment of climate change impacts on peak discharges and the PRMS and SACRAMENTO model for assessments of climate change impacts on discharge regimes. It should be mentioned that HBV only performed poorly on the criterion availability, which means there are restrictions on its use and it is not available online.

On the basis of this intercomparison, the HBV model of the Swedish Meteorological and Hydrological Institute has been chosen for implementation of the appropriate model concepts and for subsequently assessing the impact of climate change on river flooding. The dominating processes precipitation, evapotranspiration, subsurface flow and river flow are represented in the model, several sub-basins can be created to obtain the appropriate spatial scale and simulations can be done with different time steps. The processes infiltration excess overland flow, saturation excess overland flow and subsurface storm flow are represented by one fast flow component, which was found to be sufficient for this research objective. It may therefore be concluded that the fast flow component can be considered as an appropriate process instead of the separate fast flow processes. The process formulations have approximately the same level of complexity as revealed being appropriate from the literature analysis. For example, surface flow is simulated by storage routing (overland flow) and a modified version of Muskingum's

equations (river flow) implying a kinematic or diffusion wave type approach as recommended by Booij (2002a). An additional advantage of the HBV model is the large number of applications found world-wide. It has been applied in more than 30 countries including many countries in Europe and its applications cover basins in different climatological and geographical regions, ranging in size from less than 1 to more than 40,000 km² (Bergström, 1995).

The HBV model is a conceptual model of river basin hydrology which simulates river discharge using precipitation, temperature and evapotranspiration as input. The model consists of a precipitation routine representing rainfall, snow accumulation and snow melt, a soil moisture routine determining actual evapotranspiration and overland and subsurface flow, a fast flow routine representing storm flow, a slow flow routine representing subsurface flow, a transformation routine for flow delay and attenuation and a routing routine for river flow. The model version used is the HBV96 model (version 4.4). For a detailed description of HBV96, the reader is referred to SMHI (1999).

3. Observed and modelled data

3.1. Climatological data

One areally averaged temperature and one areally averaged evapotranspiration series were used as input into the river basin model. Observed station series (12 for temperature and 8 for evapotranspiration) were averaged for current climate conditions. Temperature differences between current and changed climate, simulated with the British HadCM3 general circulation model (GCM), and a relation between temperature change and evapotranspiration change (Brandsma, 1995) were taken to obtain respectively temperature and evapotranspiration series for changed climate conditions. Precipitation for current and changed climate conditions was modelled with a random cascade precipitation model (see Booij, 2002a). The discrete random cascade model of Over and Gupta (1996) has been used, because it is able to represent non-rainy areas and it can appropriately be adapted in rainfall–runoff modelling where a discrete partitioning of sub-basins exists. This model

comprises a temporal model for the complete region and a spatial model for the disaggregation of this precipitation to the appropriate scale (20 km). The temporal model consists of a discrete first-order four-state Markov chain determining precipitation occurrence and a truncated two-parameter gamma distribution describing precipitation amount. The spatial disaggregation of the temporal precipitation series is done using a discrete random cascade approach with generators determined from a beta-lognormal distribution.

The parameters of these models for current and changed climate were determined from, respectively, statistics of observed daily precipitation for the period 1970–1999 (39 stations) and modelled daily precipitation from transient runs of three GCMs and two RCMs (regional climate models). Only observed precipitation series without missing data were used, which means that half of the available number of 78 stations could not be used. The three GCMs are CGCM1 (Boer et al., 2000), HadCM3 (Gordon et al., 2000) and CSIRO9 (Gordon and O'Farrell, 1997) and the two RCMs are HadRM2 (Jones et al., 1995) and HIRHAM4 (Christensen et al., 1996). In these models, current climate conditions are represented by the period 1970–1999 and changed climate conditions are represented by the period 2070–2099 with twice the current 'equivalent' CO₂ concentration assuming an increase of 1% 'equivalent' CO₂ per year. Part of the observed and modelled precipitation statistics were downscaled to the appropriate spatial scale for precipitation of 20 km. This scale is about one-quarter of the spatial correlation length for spatially varying precipitation fields associated with the annual maximum of precipitation averaged over the whole field (see Booij, 2002b). At the 20 km scale, the bias permitted in the estimation of extreme precipitation is about 10%. At this appropriate scale, the precipitation model has generated precipitation as input into the hydrological model. Two sets of five simulations with the precipitation model were performed. In the first set, all five climate models were used to estimate average parameters for the precipitation model and five different realisations of spatially and temporally varying rainfall were generated. This does not mean that variability and extreme values are filtered out, but rather that a more stable and average scenario, representing some well-known climate

models, is obtained. In the second set, each climate model was used separately to estimate a parameter set for the precipitation model and for each parameter set (climate model) one realisation of spatially and temporally varying rainfall was generated. In this way, two sources of precipitation uncertainty can be investigated, namely the natural stochasticity and inter-model uncertainties. All relevant precipitation statistics except wet day frequency for current and changed climate were well simulated by the random cascade model.

3.2. River basin data

Elevation, soil and land use data were used in the set-up of the HBV-model. The digital elevation model (DEM) data have a horizontal resolution of 1 km and are provided by the US Geological Survey (1996). The soil data have a horizontal resolution of about 2.5 km and originate from the European Soil Bureau (King et al., 1994). These comprise soil texture and soil parent material data. The land use data have a horizontal scale of 0.25 km and are provided by the European Environmental Agency (Bossard et al., 2000). Daily discharge data at the basin outflow point (Borgharen) and at four sub-basin outflow points were employed in the simulations. More information about the data used can be found in Booij (2003).

4. Modelling issues

4.1. Different spatial model resolutions: HBV-1, HBV-15 and HBV-118

Different spatial model resolutions will be used to see the effect of model resolution on the results. In this way, a test of the appropriate model resolution can be made. The appropriate model scale requires 225–250 sub-basins. The realisation of the schematisation for the appropriate model is based on a digital elevation model and finally resulted in 118 sub-basins (HBV-118). This number of sub-basins is of the same order of magnitude and assumed to be sufficient for checking the appropriateness requirements. The HBV-118 model is compared with a model consisting of only 1 sub-basin (HBV-1) and a model with 15 sub-basins (HBV-15) following a commonly used division

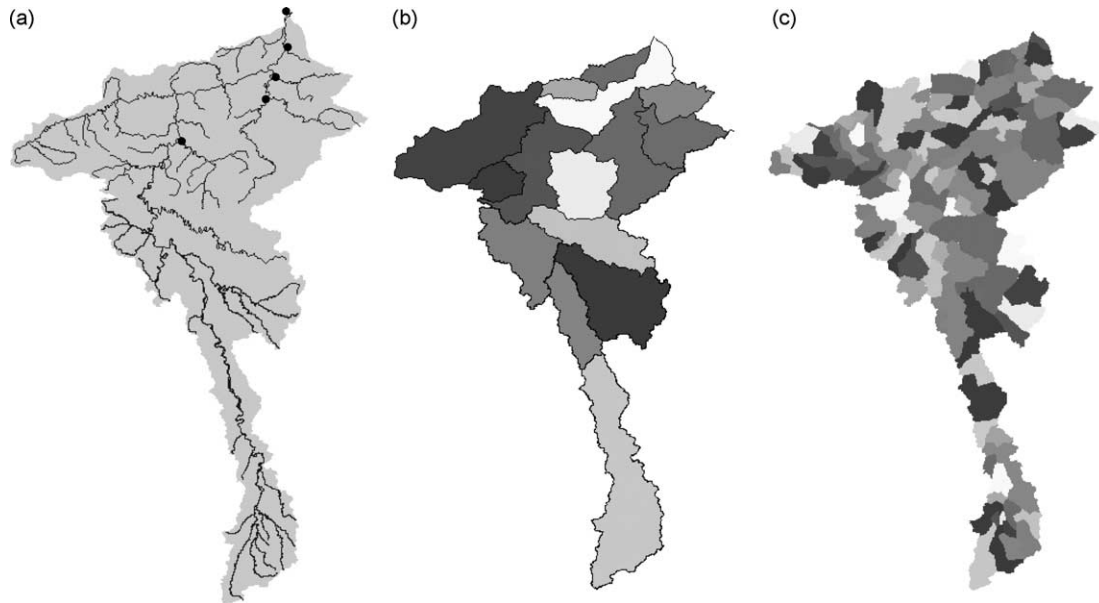


Fig. 1. Schematisations of the Meuse basin in (a) HBV-1 with points indicating discharge measuring stations, (b) HBV-15 and (c) HBV-118.

into the main sub-basins (RIZA, 2000). The three different schematisations are given in Fig. 1.

4.2. Parameter estimation

In previous HBV studies, much experience in parameter estimation has been gained and this can be used here to derive the most important parameters and to identify reasonable ranges of parameter values. The studies used are summarised

in Table 1, where some important features of each study are given. The parameter estimation consisted of three steps:

1. determination of key parameters for calibration,
2. sensitivity analysis with key parameters to obtain optimal parameter set for HBV-1 and several sub-basins of HBV-15, and
3. 'regionalisation' of these parameters to derive parameters for each sub-basin in HBV-15 and HBV-118.

Table 1
HBV modelling studies

Reference	Application area (number of basins)	Number of sub-basins	Surface area (km ²)	Calibration period	Validation period	Number of simulations
Bergström (1990)	Sweden (1)	41	$(0.3\text{--}35)\times 10^3$	1981–1986	1987–1991	
Diermanse (2001)	Mosel, Germany (1)	1 ^a	27,030	Flood events		$\sim 10^2$ -SA ^b
Harlin and Kung (1992)	Sweden (2)	1	1370–4483	18–20 years		$\sim 10^3$ -MC ^c
Krysanova et al. (1999)	Elbe, Germany (1)	1–44	$(1\text{--}81)\times 10^3$	1981–1983	1984–1989	
Lindström et al. (1997)	Sweden (7–10)	1	174–5975	10 years	10 years	
Seibert (1999)	Sweden (11)	1	7–950	1981–1990		$\sim 10^5$ -MC
Uhlenbrook et al. (1999)	Brugga, Ger. (1)	1	40	1975–1984		$\sim 10^5$ -MC

Surface area indicates area of the sub-basins in the case of distributed HBV versions (number of sub-basins > 1).

^a One parameter (FC) was 'fully distributed' into 27×10^3 different values (1 km² scale), precipitation gauge density and precipitation averaging effect was assessed.

^b SA, sensitivity or similar analysis.

^c MC, Monte Carlo analysis.

Steps 1 and 2 are briefly described below, step 3 is described in the next section.

The most important and uncertain parameters occur in the soil moisture and fast flow routine. The main parameters in the soil moisture routine are FC (maximum soil moisture storage in millimeter), LP (fraction of FC above which potential evapotranspiration occurs and below which evapotranspiration will be reduced) and BETA (determining the relative contribution to runoff from a millimeter of precipitation at a given soil moisture deficit). The main parameters in the fast flow routine are α (measure of non-linearity for fast flow; for $\alpha=0$, fast flow is the outflow from a linear reservoir and for $\alpha>0$, fast flow becomes more and more non-linear), Q_H (geometric mean of mean discharge and mean annual maximum discharge) and k_H (recession coefficient at Q_H). Values and ranges of these parameters used in the studies from Table 1 and two additional studies are given in Table 2.

In the second step, multiple sensitivity analyses for these parameters have been performed. Table 2 has been used to determine the parameter ranges for

the multiple sensitivity analyses (SA) for HBV-1. Additional univariate sensitivity analyses were done for four sub-basins of HBV-15 (Lesse, Ourthe, Amblève and Vesdre) with overall parameter ranges and values given in Table 2 as well.

The optimality of the model output (discharge) is assessed in different ways, namely by applying the Nash–Sutcliffe efficiency coefficient R^2 (Nash and Sutcliffe, 1970), the relative volume error RVE and the relative extreme value error REVE

$$R^2 = 1 - \frac{\sum_{i=1}^N [Q_m(i) - Q_o(i)]^2}{\sum_{i=1}^N [Q_o(i) - \bar{Q}_o]^2} \quad (1)$$

$$\text{RVE} = 100 \frac{\sum_{i=1}^N [Q_m(i) - Q_o(i)]}{\sum_{i=1}^N Q_o(i)} \quad (2)$$

$$\text{REVE}(T) = 100 \frac{\text{RV}_m(T) - \text{RV}_o(T)}{\text{RV}_o(T)} \quad (3)$$

where i is the time step, N is the total number of time steps, Q is the discharge and subscripts ‘o’ and ‘m’ means observed and modelled. $\text{RV}(T)$ is the T -year return value determined by fitting a Gumbel

Table 2

Parameter values and ranges from the studies in Table 1, Killingtveit and Sæthun (1995), SMHI (1999) and HBV-1, HBV-15 and HBV-118

Reference	FC (mm)	LP (–)	BETA (–)	α^a (–)	k_H^a (day ^{–1})	$Q_H^{a,b}$ (mm day ^{–1})
Bergström (1990)	100–300	0.50–1.0	1.0–4.0			
Diermanse (2001)	0–580	0.80	3.0			
Harlin and Kung (1992)	50–274	0.73–1.0	1.0–5.9			
Killingtveit and Sæthun (1995)	75–300	0.70–1.0	1.0–4.0			
Krysanova et al. (1999)	220–391	0.70	2.0			
Seibert (1999)	50–500	0.30–1.0	1.0–6.0			
SMHI (1999) ^c	200	0.9	2.0	1.0	0.17	3.0
Uhlenbrook et al. (1999)	100–550	0.30–1.0	1.0–5.0			
HBV-1 (SA)	200–500	0.2–0.8	1.0–3.0	0.1–1.1	0.06–0.11	
HBV-15 (SA)	100–400	0.2–0.8	1.0–3.0	0.8–1.1	0.08–0.15	
HBV-1 (optimal values)	340	0.34	1.0	0.7	0.074	2.22
HBV-15 (optimal values)						
Lesse	253	0.65	1.5	0.7	0.095	3.02
Ourthe	180	0.71	1.5	1.1	0.12	3.27
Amblève	202	0.68	1.9	0.9	0.11	4.15
Vesdre	350	0.68	1.3	1.1	0.14	3.79
HBV-15 (regionalisation)	180–384	0.28–0.71	1.0–2.3	0.2–1.1	0.06–0.14	1.69–4.30
HBV-118 (regionalisation)	185–660	0.28–0.71	1.2–2.1	0.1–1.9	0.07–0.17	1.69–4.30

^a In the fast flow routine of HBV96 α , k_H and Q_H are used, while in older versions of HBV one or more recession coefficients k_i were directly used (without α). Therefore, comparisons between the fast flow routine parameters in the two versions cannot be made.

^b Q_H can be directly determined from measured discharges and has not been calibrated.

^c Default values for HBV96.

distribution to annual maximum values and extrapolating this distribution to T -year return values (20 and 100 years). Furthermore, visual inspections of the observed and simulated hydrographs should always accompany model experiments. Since the soil moisture routine parameters particularly influence the discharge volume, the criteria for the multiple sensitivity analysis with FC, LP and BETA are RVE and R^2 . On the other hand, the fast flow routine parameters particularly affect the shape of the hydrograph and extreme discharges and therefore R^2 and REVE are used as criteria in the bivariate sensitivity analysis with α and k_H .

4.3. Regionalisation

The HBV-15 and HBV-118 models cannot be calibrated in the same way as the HBV-1 model, because additional observed discharges for the sensitivity analyses are only available for four sub-basins. It is therefore necessary to determine the key parameters of the other sub-basins in an alternative way. The concept of ‘regionalisation’ is used for this purpose. This involves the use of relationships between key parameters and river basin characteristics (e.g. land use, soil type) to assess the parameter values for the remaining sub-basins. These relationships can be established by employing the calibrated parameters from the sensitivity analyses and the corresponding basin characteristics or using relationships from literature. Separate relationships for each key variable or for example Hydrological Response Units (HRUs) representing hydrologically similar areas (e.g. Kite and Kouwen, 1992) can be used for this purpose. The separate relationships for the five key parameters in HBV-15 and the regionalisation for HBV-118 are described below. The regionalisation relationships are used to distribute the parameter values for the sub-basins of HBV-15 around the mean parameter values as obtained for HBV-1 and the parameter values for the sub-basins of HBV-118 around the (eventually adjusted) mean parameter values as obtained for HBV-15 and thus introducing spatial variability of the parameters. The basin characteristics used are assumed to indicate at least the direction of variation of a particular parameter.

The soil moisture routine parameters FC and LP are relatively scale independent (Bergström and

Graham, 1998) and can be used at all covered scales (~ 100 – $20,000$ km²). This is in the same range as the scales in Bergström (1990). Parameter FC is the maximum capacity of the soil to hold water and is related to soil properties as the soil moisture content at wilting point, the porosity and the soil depth. Here, the FC from HBV-1 is distributed taking into account the calibrated FC values from the four sub-basins in HBV-15 and using the volumetric soil moisture content at wilting point θ_w and the soil porosity ϕ (data on soil depths were not available)

$$FC \sim \phi - \theta_w \quad (4)$$

Parameter LP is the fraction of FC above which potential evapotranspiration occurs. It is assumed to be dependent on the volumetric soil moisture content at wilting point θ_w and field capacity θ_f and on the soil porosity ϕ to account for the dependency of LP on FC

$$LP \sim \frac{\phi - \theta_w}{\theta_f - \theta_w} \quad (5)$$

Parameter BETA describes how the runoff coefficient increases as the maximum soil moisture content FC is approached. This parameter can be regarded more as an index of heterogeneity than a measure of soil properties (Bergström and Graham, 1998). This is because for low values runoff is gradually generated, indicating heterogeneous conditions, whereas for high values runoff is simultaneously generated, implying homogeneous conditions. In general, this means for large sub-basins with much heterogeneity smaller values for BETA than for small sub-basins with relatively little variability. Seibert (1999), on the other hand, found an increase of BETA values with sub-basin area A , although his relation was weak. The former explanation (increasing BETA values with decreasing area) will serve as a basis for a BETA–area relationship, because it is physically more plausible

$$BETA \sim \frac{1}{A} \quad (6)$$

Parameter α is a measure of the non-linearity of the fast flow process. Small sub-basins with steep hills and low permeable soils will generally result in more non-linearity in the fast flow mechanisms than large sub-basins with flat terrains and high permeable soils. The calibrated α values were found to be most

dependent on slope S_0 rather than on surface area or soil type

$$\alpha \sim S_0 \tag{7}$$

Parameter k_H is a recession coefficient at high flow rate Q_H and can be approximated by estimating the recession coefficient from an observed hydrograph at flow rate Q_H (SMHI, 1999). This parameter is influenced by similar factors as α and calibrated k_H

values were found to be most dependent on slope S_0 as well

$$k_H \sim S_0 \tag{8}$$

Results of the regionalisation are given in Fig. 2, where regionalisation relations for the five HBV parameters with calibrated and regionalised values are given. The relations between the parameters and their indicators are poor (k_H and LP) to moderate

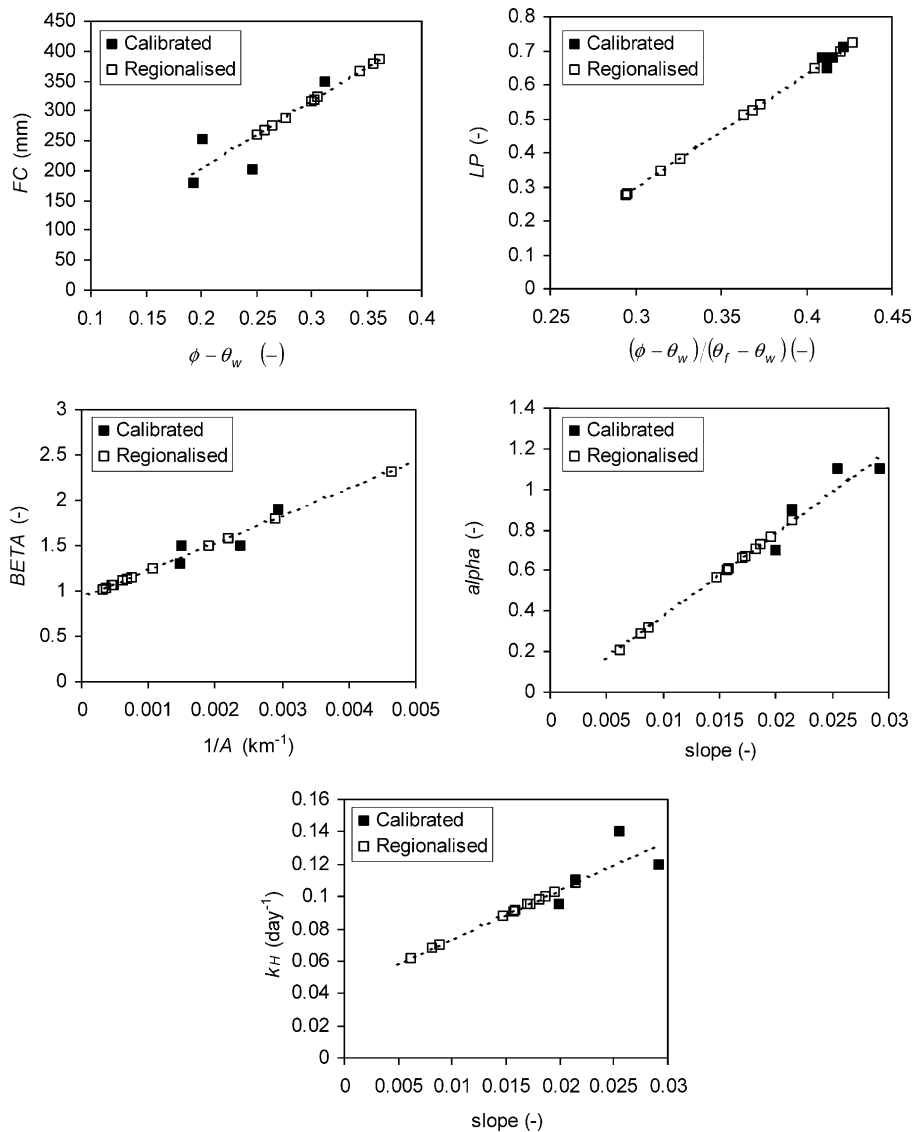


Fig. 2. Regionalisation relations for five HBV parameters (FC, LP, BETA, α (alpha) and k_H) with calibrated and regionalised values for HBV-15 (see also Table 2).

Table 3
Description of climatic input for model experiments

	Precipitation	Temperature	Evapotranspiration
Calibration	Stations (39) 1970–1984	Stations (12) 1970–1984	Stations (8) 1970–1984
Validation	Stations (39) 1985–1996	Stations (12) 1985–1996	Stations (8) 1985–1996
Current climate	Random Cascade Model (76), 30 years, 5 realisations ^a	Stations (12) 1967–1996	Stations (8) 1967–1996
Changed climate	Random Cascade Model (76), 30 years, 10 realisations ^b	Stations + change (12) 1967–1996	Stations + change (8) 1967–1996

^a Five realisations using the same precipitation model parameters for HBV-1 and HBV-15, one realisation for HBV-118.

^b Five realisations using the same precipitation model parameters (natural stochasticity) and five realisations using parameters derived from each model separately (3 GCMs and 2 RCMs; inter-model uncertainty) for HBV-1 and HBV-15, one realisation for HBV-118.

(FC and BETA) and reasonable (α). It should be noted that only four calibrated values for each parameter (from four sub-basins) have been used to estimate the regionalisation relations and thus the parameters of the remaining eleven sub-basins. This introduces a lot of uncertainty, which may be amplified by extrapolation of the regionalisation relations outside their calibrated ranges (in particular for LP and α). Therefore, care should be taken in applying these relations to other areas.

The regionalisation for seven variables (additionally Q_H and Q_{perc}) in HBV-118 is described in detail by Van der Wal (2001). He used only one indicator based on the slope, the soil texture and the soil parent material representing the reaction behaviour of the sub-basin to distribute the seven key parameters among the 118 sub-basins. For this purpose, the three characteristics were each divided into three categories representing a fast, medium or slow reaction behaviour. For example, areas with slopes larger than 3.6% are characterised as fast, between 1.4 and 3.6% as medium and smaller than 1.4% as slow. The resulting categorisation for each characteristic was quantified using three values -1 (fast), 0 (medium)

and 1 (slow). Finally, the indicator for each sub-basin was obtained by summing the values for each characteristic and thus obtaining a range for this indicator between -3 and 3 . The indicator has been used to vary the parameter values of the HBV-118 sub-basins around the (eventually adjusted) mean parameter values as obtained for HBV-15 through a similar calibration procedure as explained in Section 4.2. The resulting parameter ranges are given in Table 2.

4.4. Model experiments

The impact of climate change on river flooding is assessed with HBV-1, HBV-15 and HBV-118 in four steps. These four steps are the calibration described above, the validation, the simulation under current climate conditions with synthetic precipitation and the simulation under changed climate conditions with synthetic precipitation. A description and summary of the climatic input for the four steps are summarised in Tables 3 and 4, respectively. Information about the model experiments with HBV-1, HBV-15 and HBV-118 is given in Table 5.

Table 4
Summary of climatic input for model experiments

	Precipitation (20 km scale)		Temperature (areally averaged)		Evapotranspiration (areally averaged)	
	Average (mm)	Standard deviation (mm)	Average (°C)	Standard deviation (°C)	Average (mm)	Standard deviation (mm)
Calibration	2.6	4.8	8.7	6.4	1.8	1.6
Validation	2.7	5.2	9.0	6.7	1.9	1.7
Current climate	2.7–2.9	4.9–5.1	8.8	6.5	1.8	1.6
Changed climate						
Stochasticity	2.7–3.0	5.7–6.0	12.5	7.4	2.1	1.9
Inter-model uncertainty	2.1–2.9	5.2–6.4				

Table 5
Model experiments with HBV-1, HBV-15 and HBV-118

	HBV-1	HBV-15	HBV-118
Calibration	Discharge (1) 1970–1984	Discharge (5), regionalisation, 1970–1984	Discharge (5), regionalisation, 1970–1984
Validation	Discharge (1) 1985–1996	Discharge (5) 1985–1996	Discharge (5) 1985–1996
Current climate	Discharge (1), 30 years, 5 realisations	Discharge (5/15), 30 years, 5 realisations	Discharge (5/118), 30 years, 1 realisation
Changed climate	Discharge (1), 30 years, 5 realisations	Discharge (5/15), 30 years, 10 realisations	Discharge (5/118), 30 years, 1 realisation

The point precipitation series from stations are interpolated using Thiessen polygons. These areally averaged precipitation series are combined with the HBV-1, HBV-15 and HBV-118 schematisations from Fig. 1 to obtain areally averaged precipitation series for 1, 15 and 118 sub-basins, respectively. The areally averaged random cascade precipitation series are combined with the HBV-1, HBV-15 and HBV-118 schematisations in the same way.

5. Climate change impact on river flooding in the Meuse basin

5.1. Calibration

The optimal values for the soil moisture routine parameters were obtained by requiring that RVE should be less than 1% and R^2 should be as high as possible. The optimum values are poorly defined and are given in Table 2. A similar approach has been conducted for the fast flow routine parameters by requiring that REVE should be less than 10% and R^2 should be as high as possible. The resulting α and k_H values are given in Table 2 as well. During these sensitivity analyses, the values of the other (less important) parameters were kept at pre-determined values based on univariate sensitivity analyses and the studies mentioned in Table 1. The calibrated parameter values are generally within the ranges from other studies. The value for the parameter LP is low, which means that potential evapotranspiration occurs already under relatively dry conditions. Although this could yield an overestimation of the total evapotranspiration, observed and simulated water balances compared favourably. The optimal values of the soil moisture and fast flow routine parameters for the four

sub-basins (Lesse, Ourthe, Amblève and Vesdre) are summarised in Table 2 as well.

The optimal parameter values for HBV-1 and the four sub-basins of HBV-15 together with θ_w , θ_f and ϕ -values based on soil texture (Rawls et al., 1993), S_0 values based on elevation data and A values are used to quantify the regionalisation relationships from Eqs. (4)–(8). Finally, these equations have been used to determine the parameters values for the remaining 11 sub-basins (see Table 2).

Next, the results obtained with the chosen parameter values for HBV-1, HBV-15 and HBV-118 can be compared. Therefore, Fig. 3 shows the daily discharge at Borgharen for one arbitrary year (1984) with a considerable peak for the observed and HBV-1, HBV-15 and HBV-118 simulated situation. The observed hydrograph is simulated realistically by all three models, although the performance becomes somewhat better with an increasing number of sub-basins. Fig. 4 gives the extreme value distribution of annual extremes for the observed and simulated series. Most striking feature is the good simulation by HBV-15 and HBV-118, but also by HBV-1. The resulting criteria R^2 , RVE [by means of average] and REVE [by means of RV(100)] together with the standard deviation of daily discharges are summarised in Table 6. This table mainly confirms the findings from the visual inspection; the good simulation of average discharge behaviour illustrated by high R^2 values and the proper simulation of extremes (difference is negligible for HBV-15 and HBV-118).

5.2. Validation

In the validation, the parameter values are kept the same as in the calibration, but the simulations are repeated with other, independent input series

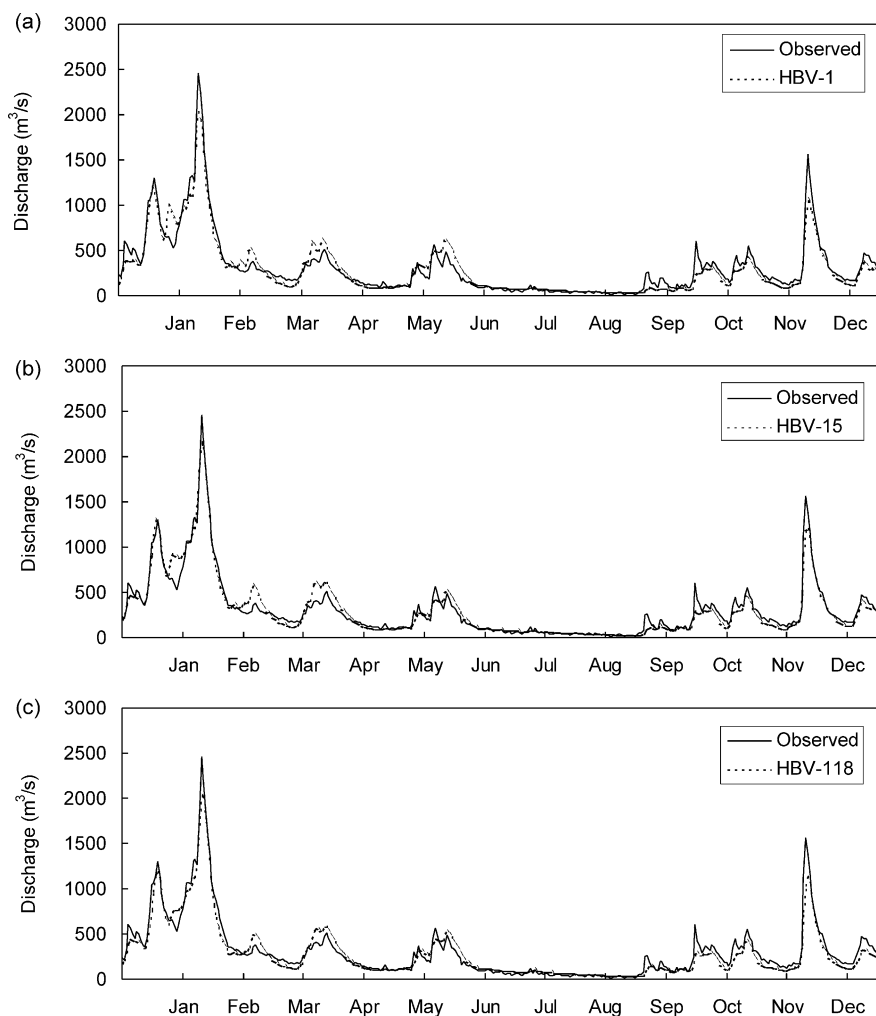


Fig. 3. Observed and simulated discharge for 1984 for (a) HBV-1, (b) HBV-15 and (c) HBV-118.

(see Tables 3 and 5). The results are shown in Figs. 5 and 6 and Table 6. Fig. 5 shows the daily discharge at Borgharen for December 1993 through March 1995 with two considerable peaks for the observed and HBV-15 and HBV-118 simulated situation. The observed hydrograph is simulated realistically by the two models, even better than in the calibration. Fig. 6 gives the extreme value distribution of annual extremes for the observed and simulated series. Again the extreme value distribution is well simulated by all models. The resulting criteria R^2 , RVE and REVE and the standard deviation of daily discharges at Borgharen are summarised in Table 6. Additionally, Table 7 gives R^2 , RVE and REVE for

the calibration and validation for the four sub-basins. The differences between average discharge behaviour of the sub-basins modelled by HBV-15 and HBV-118 are small. Extreme discharges are generally better simulated by HBV-118 in the calibration, where in the validation HBV-15 is a bit better. This also shows that the regionalisation method only slightly influences the model performance, although this performance is dependent on, e.g. the spatial resolution of precipitation as well. More discharge measurements could possibly show in future the advantages and/or disadvantages of HBV-118 with respect to HBV-15 as well as the preference of one regionalisation method over another.

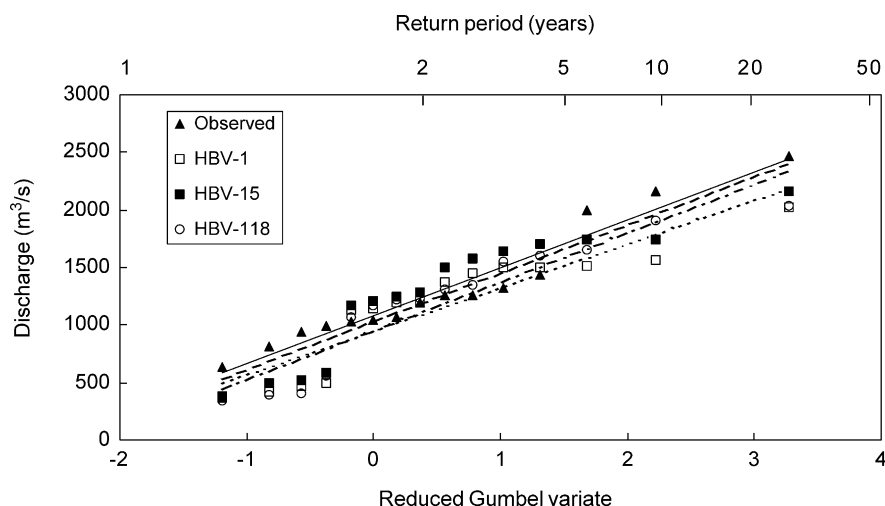


Fig. 4. Gumbel plot for annual maximum discharges for the period 1970–1984, observed and simulated with HBV-1, HBV-15 and HBV-118. Regression lines for observed (solid), HBV-1 simulated (dotted), HBV-15 simulated (dashed) and HBV-118 simulated (dashed-dotted) are also shown.

5.3. Synthetic current climate

The results of the random cascade model for the current climate are used as input in HBV-1, HBV-15 and HBV-118 to simulate daily discharge series for the current climate (see Table 5). Fig. 7 shows

the cumulative frequency distribution of daily discharges for the observed series and five realisations with HBV-1 and HBV-15 and one realisation with HBV-118 for current climate. The only realisation with HBV-118 is the maximum one in terms of HBV-15 extreme discharges. Fig. 8 gives the extreme value

Table 6

Results from calibration, validation and simulations with precipitation model for current and changed climate

		R^2 (-)	Average		Standard deviation		RV(100)	
			Value ($\text{m}^3 \text{s}^{-1}$)	RVE ^a (%)	Value ($\text{m}^3 \text{s}^{-1}$)	Diff. ^a (%)	Value ($\text{m}^3 \text{s}^{-1}$)	REVE ^a (%)
Calibration	Observed	–	222	–	252	–	2929	–
	HBV-1	0.85	222	0	251	0	2719	–7
	HBV-15	0.87	231	+4	270	+7	2977	+2
	HBV-118	0.88	224	+1	255	+1	2896	–1
Validation	Observed	–	235	–	300	–	3703	–
	HBV-1	0.91	238	+1	307	+2	3817	+3
	HBV-15	0.92	244	+4	324	+8	4008	+8
	HBV-118	0.93	239	+2	303	+1	3772	+2
Synthetic current climate	Observed	–	229	–	275	–	3292	–
	HBV-1	–	232–266	+1/+16	265–296	–4/+8	2553–3236	–22/–2
	HBV-15	–	237–271	+3/+18	275–306	0/+11	2621–3226	–20/–2
	HBV-118	–	244	+6	264	–4	2958	–10
Synthetic changed climate	HBV-1	–	204–264	–12/–1	253–334	–5/+13	2426–3565	–5/+10
	HBV-15	–	207–266	–13/–2	260–344	–5/+12	2591–3661	–1/+13
	HBV-118	–	258	+6	314	+19	3354	+13
Uncertainty	HBV-15	–	208–244	–12/–10	270–299	–2/–2	2551–3530	–3/+9

^a Difference (diff.) in % with respect to the corresponding observed (calibration, validation, synthetic current climate) or simulated (synthetic changed climate) value.

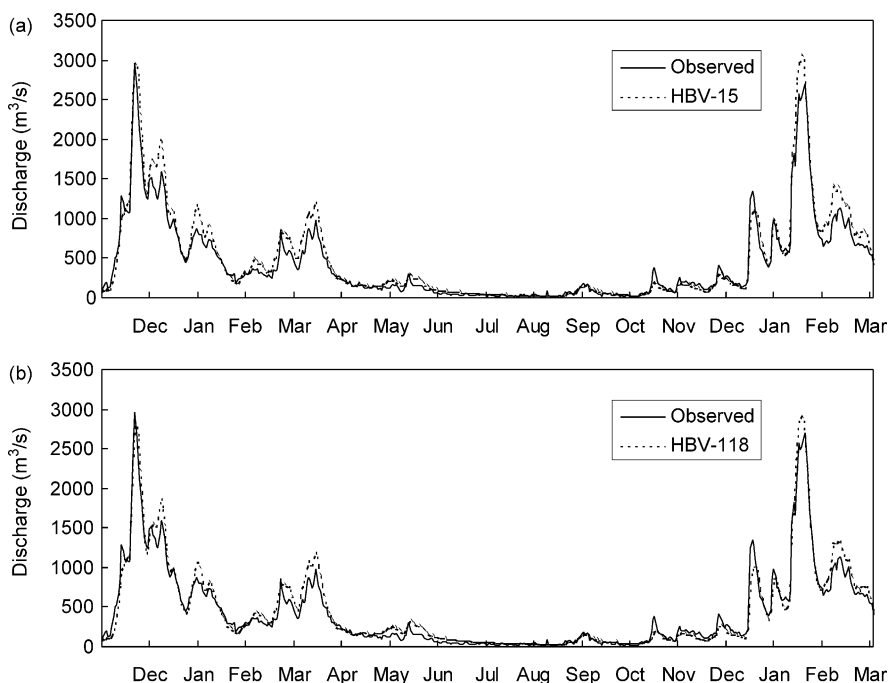


Fig. 5. Observed and simulated discharge at Borgharen for December 1993–March 1995 for (a) HBV-15 and (b) HBV-118.

distribution of annual extremes for the observed and simulated series. The five realisations are quantified in Table 6 by means of the average and standard deviation of daily discharges and the 100-year return value $RV(100)$.

The general trend from these figures and table is a small overestimation of the average and standard deviation (variability) of discharges and a considerable underestimation of extreme discharges in the case of HBV-1 and HBV-15. HBV-118 slightly

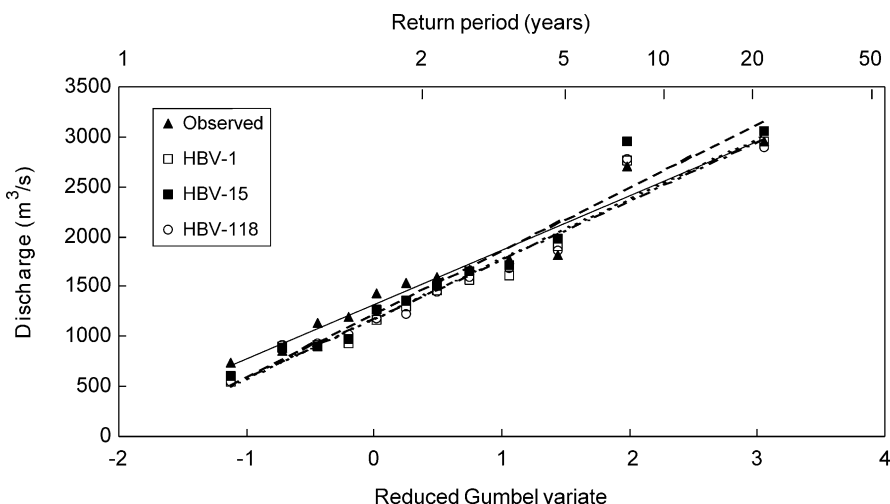


Fig. 6. Gumbel plot for annual maximum discharges for the period 1985–1996 as observed and simulated with HBV-1, HBV-15 and HBV-118. Regression lines for observed (solid), HBV-1 simulated (dotted), HBV-15 simulated (dashed) and HBV-118 simulated (dashed-dotted) are shown as well.

Table 7
Results for tributaries from calibration and validation of HBV-15 and HBV-118

		Calibration			Validation		
		R^2 (-)	Average RVE ^a (%)	RV(100) REVE ^a (%)	R^2 (-)	Average RVE ^a (%)	RV(100) REVE ^a (%)
Lesse	HBV-15	0.88	0	-10	0.89	+7	-23
	HBV-118	0.88	+1	+2	0.91	+9	-21
Ourthe	HBV-15	0.80	+1	-10	0.86	+4	-3
	HBV-118	0.87	+1	-4	0.92	+4	+4
Amblève	HBV-15	0.80	+1	-12	0.87	+5	-2
	HBV-118	0.78	+3	-2	0.84	+7	+7
Vesdre	HBV-15	0.80	0	-39	0.76	-4	+1
	HBV-118	0.77	+2	-23	0.76	0	+18

^a Difference in % with respect to the corresponding observed value.

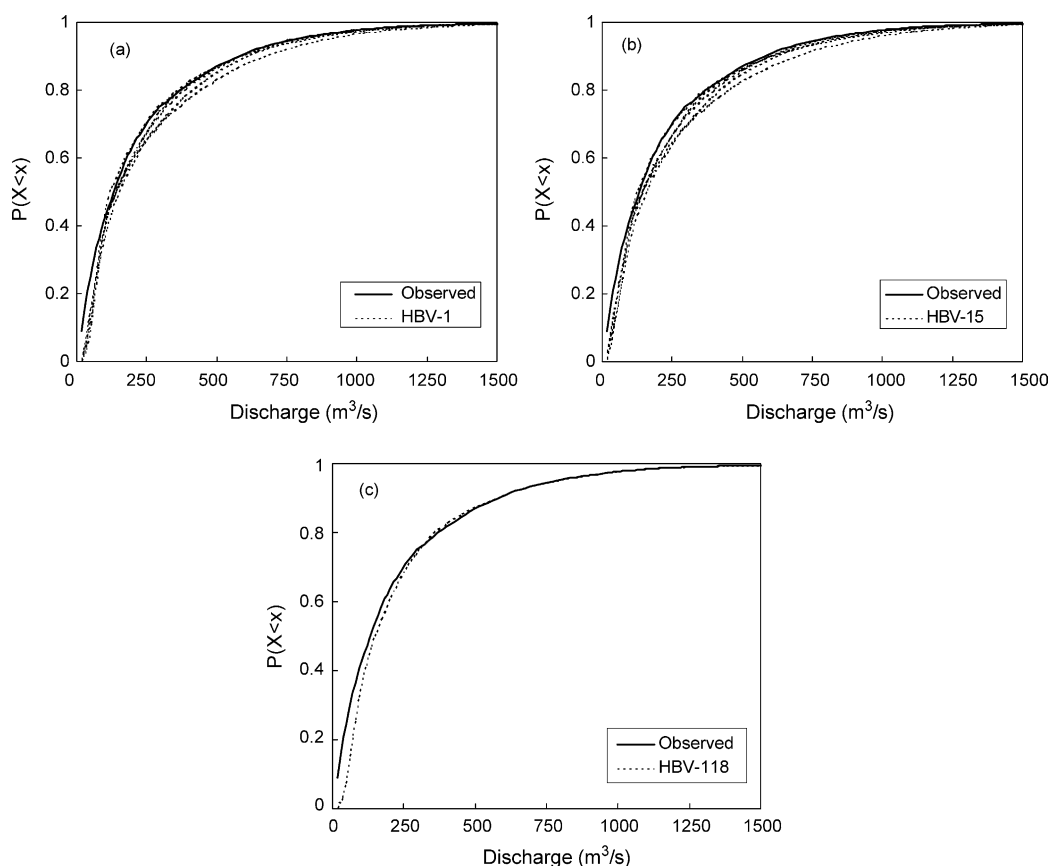


Fig. 7. Cumulative frequency distribution $P(X < x)$ for daily discharges up to $1500 \text{ m}^3 \text{ s}^{-1}$ for 30 years under current climate conditions for (a) observed series and five precipitation realisations with HBV-1, (b) observed series and five precipitation realisations with HBV-15 and (c) observed series and one precipitation realisation with HBV-118.

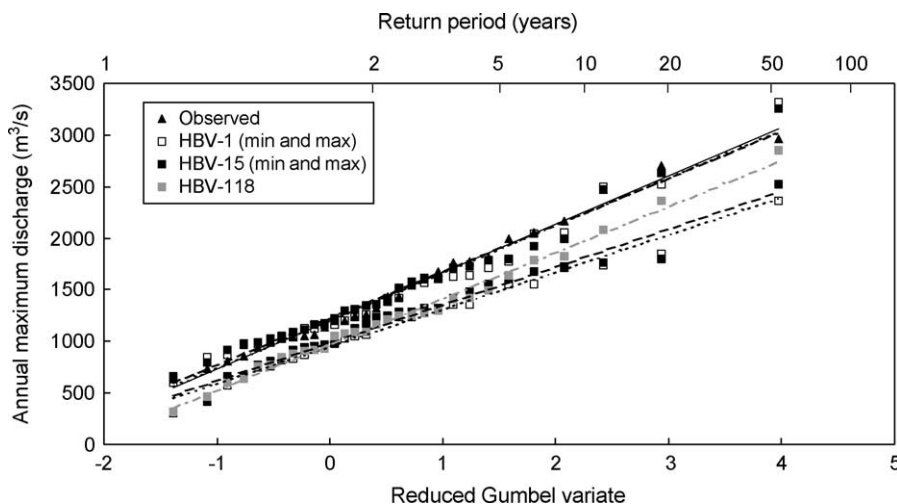


Fig. 8. Gumbel plot for annual maximum discharges for a 30-year period as observed (1970–1999) and simulated with five precipitation realisations for HBV-1 and HBV-15 and one precipitation realisation for HBV-118 under current climate conditions. Only the minimum and maximum of the five HBV-1 and HBV-15 realisations are shown. Regression lines for observed (solid), HBV-1 simulated (dotted), HBV-15 simulated (dashed) and HBV-118 simulated (grey dashed-dotted) are given as well.

underestimates the discharge variability and underestimates extreme discharges with respect to HBV-15. However, a general tendency for HBV-118 is hard to identify, because only one precipitation realisation has been used for HBV-118. The small overestimation of average discharge behaviour can be explained by the small overestimation of average precipitation behaviour by the random cascade model (see Booij, 2002a; on average +8% for mean precipitation and +4% for the standard deviation of daily precipitation). However, the underestimation of extreme discharges by HBV-1 and HBV-15 cannot be

explained by the statistics of the precipitation input. The random cascade model rather overestimates than underestimates extreme precipitation.

The main cause of this underestimation can be found in the transformation of observed precipitation at the point scale and simulated precipitation at the 20 km scale to areally averaged precipitation at the basin (HBV-1, ~150 km) or sub-basin scale (HBV-15, ~40 km and HBV-118, ~13 km). This is illustrated in Table 8 where the important statistics from the precipitation model results at the HBV-15 and HBV-118 sub-basin scales for the observed

Table 8

Daily precipitation statistics at the sub-basin scale for observed and random cascade modelled current climate

Sub-basin scale statistics	HBV-15			HBV-118		
	Observed	Modelled	Diff. (%) ^a	Observed	Modelled	Diff. (%) ^a
Average (mm)	2.6	2.7	+4	2.6	2.7	+4
Standard deviation (mm)	4.8	4.6	-4	5.0	4.9	-2
Wet day frequency (-)	0.57	0.59	+3	0.53	0.51	-4
Temporal correlation cf. lag-1 (-)	0.31	0.29	-4	0.28	0.27	-4
20-year return value (mm)	53.6	51.7	-4	57.6	55.4	-4
100-year return value (mm)	66.3	63.7	-4	71.5	68.4	-4
5-day 100-year return value (mm)	136	109	-20	139	117	-16
8-day 100-year return value (mm)	173	139	-19	174	147	-15
10-day 100-year return value (mm)	193	158	-18	194	164	-15

^a Difference in % between modelled and observed statistic.

and simulated situation (one realisation with REVE $\approx -20\%$) are summarised. In particular, the 5-day, 8-day and 10-day 100-year precipitation return values are underestimated by the precipitation model at the HBV-15 (by about 20%) and HBV-118 (by about 15%) sub-basin scale, but also 1-day extreme values and the standard deviation are underestimated compared to the 20 km scale (where the precipitation model mainly overestimates these statistics, see also Booij, 2002a). This underestimation of generated extreme precipitation at the sub-basin scale is in fact an overestimation of observed extreme precipitation at the sub-basin scale. Namely, the observed 5-day, 8-day and 10-day 100-year precipitation return values in Table 8 are approximately the corresponding observed point values.

The overestimation of the standard deviation (variability) and extreme behaviour of observed precipitation is explained by the fact that for a lot of sub-basins, in particular for HBV-118, only one or two stations are used as precipitation input into the model. This results in observed input at the point scale compared to simulated input at the (correct) 20 km scale. Observed precipitation is considered as areally averaged precipitation, but is actually point precipitation. Consequently, observed precipitation shows too much variability and extreme behaviour, which will have implications for the parameter estimation during calibration. Parameters are estimated under too variable and extreme conditions, which may have consequences for simulations under changed conditions (e.g. land use and climate change). Unfortunately, insufficient precipitation stations are available to assess the areally averaged sub-basin scale precipitation in a right way and therefore this overestimation has occurred. The overestimation of precipitation variability and extreme behaviour seems to be common practice, because in most rainfall-runoff modelling studies station precipitation is used as input in stead of areally averaged precipitation at the sub-basin scale.

The difference between HBV-15 and HBV-118 in Table 8 (-20 and -15%) can be explained by the fact that modelled precipitation is less averaged when transformed to the HBV-118 scale than when transformed to the HBV-15 scale. However, the difference in discharge 100-year return values for the HBV-15 and HBV-118 model using the same

(maximum) precipitation realisation (-2 and -10% , respectively in Table 6) cannot be explained by these differences in precipitation at the sub-basin scale. This difference may be caused by differences in regionalisation techniques and related differences in parameter values (e.g. FC values in Table 2 cover a much broader range in the case of HBV-118). In this way, it gives some information about uncertainties due to parameter estimation, but it does not give information about uncertainties due to differences in processes incorporated or process formulations. Nevertheless, the calibration and validation results from HBV-15 and HBV-118 were comparable. Fig. 8 shows a large difference (range) between the minimum and maximum of the modelled realisations (about 20%), which illustrates the large impact of the stochasticity of the precipitation process.

5.4. Synthetic changed climate

The climate change situation will be considered by comparing the results obtained with input from the precipitation model for current and changed climate conditions. Fig. 9 shows the cumulative frequency distribution of daily discharges for five realisations with HBV-1 and HBV-15 and one realisation with HBV-118 for the current and changed climate. Fig. 10 gives the 20-year and 100-year return values for the current and changed climate. Quantitative figures are shown in Table 6.

The general trend is a small decrease of the average discharge and a small increase of the standard deviation of the discharge (variability) and extreme discharges with climate change. The decrease of the average discharge has to do with the slight increase of modelled average precipitation with climate change (about 5%) combined with the considerable increase of (potential) evapotranspiration (on average about 15%, see Table 4). The increase in discharge variability and extreme discharges is the result of the considerable increase of precipitation variability and extreme precipitation (10–20%), but is less than would be expected on the basis of the changes in precipitation behaviour. There are even precipitation realisations which have resulted in a small decrease of the extreme value distribution for annual discharges derived from both HBV-1 and HBV-15. As a consequence of this, the range in extreme values has

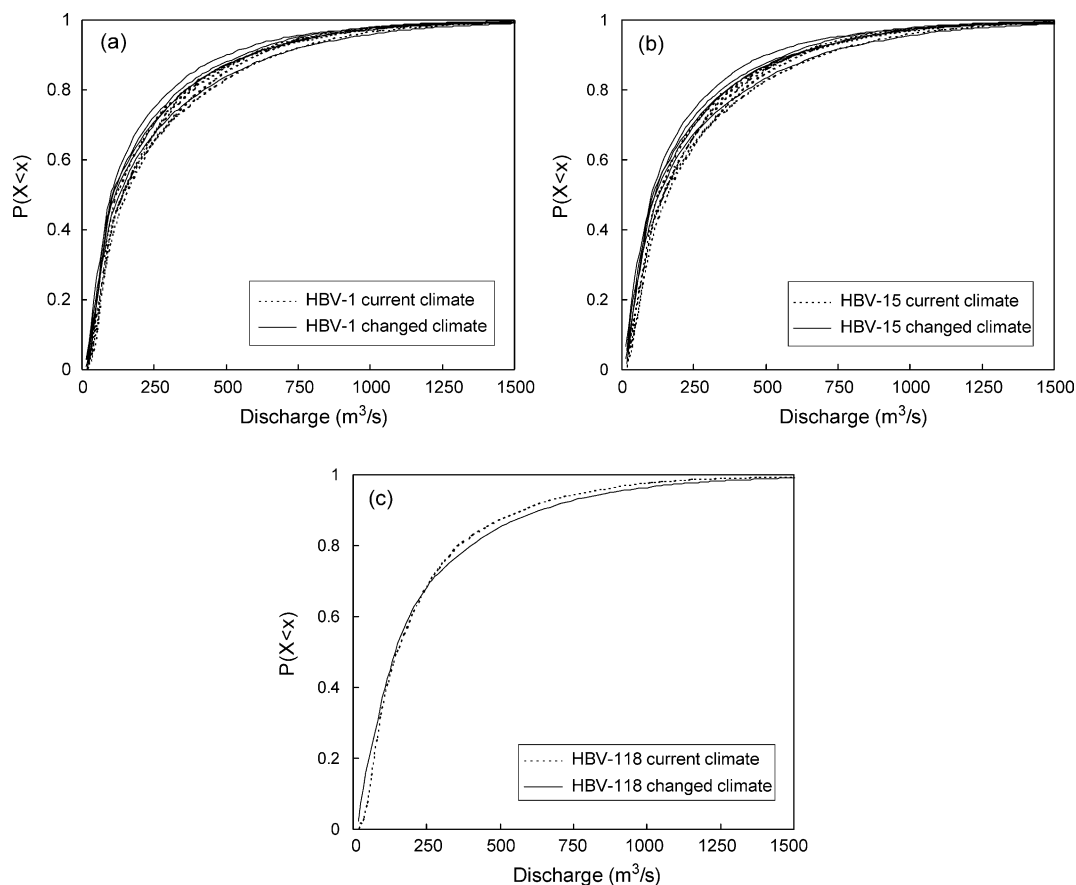


Fig. 9. Cumulative frequency distribution $P(X < x)$ for daily discharges up to $1500 \text{ m}^3 \text{ s}^{-1}$ under current and changed climate conditions for five realisations of 30 years for (a) HBV-1 and (b) HBV-15 and one realisation of 30 years for (c) HBV-118.

increased with respect to the simulations for current climate conditions. The HBV-118 model shows a similar increase in 20-year and 100-year return values with climate change as the corresponding realisations for HBV-1 and HBV-15.

When using the HBV model for the assessment of climate change impacts, it has been assumed that the model is valid outside its calibration conditions. This is partly checked in the validation step, where the climatic input is more variable (see Table 4) resulting in more variable and extreme discharge behaviour (e.g. the 100-year return value in the validation period is 25% larger than in the calibration period). However, the HBV model versions showed even better results in the validation step than in the calibration step. Moreover, simulated extremes with climate change are of the same order of magnitude as the extremes in

the calibration and validation periods. It is not expected that rainfall–runoff processes in the HBV model and corresponding parameters will change considerably during these climate change conditions. Obviously, other possible changes such as land use changes or river restoration may require model and/or parameter changes, but this will also be the case for current climate conditions.

5.5. Uncertainties

The uncertainty in extreme discharges with climate change is caused by various sources of uncertainty of which the most important are: climatological input (precipitation, evapotranspiration), model structure, parameter values and extrapolation to large return periods.

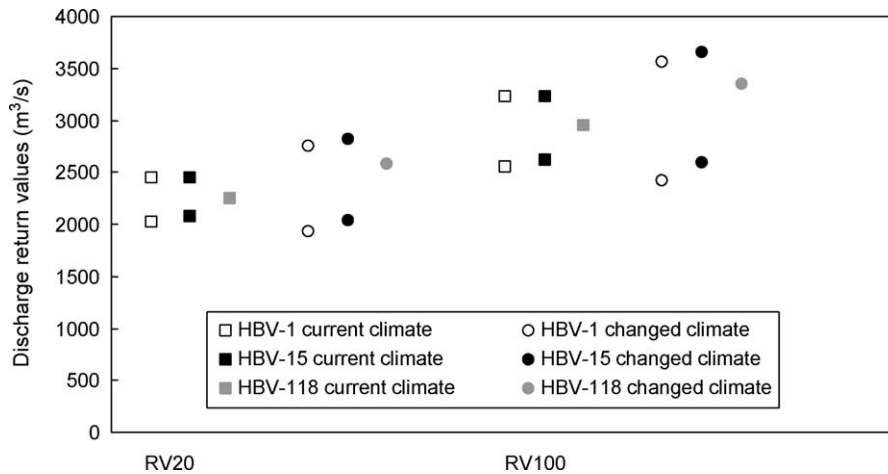


Fig. 10. Discharge 20-year (RV20) and 100-year (RV100) return values from a 30-year period as simulated with five precipitation realisations for HBV-1 and HBV-15 and one precipitation realisation for HBV-118 under current and changed climate conditions. Only the minimum and maximum of the five HBV-1 and HBV-15 realisations are shown.

The uncertainty in the modelled standard deviation of precipitation and extreme precipitation with climate change was found to be large in Booij (2002b), 30–50%. This uncertainty consisted of climate model errors (differences between observed and modelled climate), inter-model differences and an estimation of climate forcing uncertainties. The effect of inter-model differences on extreme river discharges

has been roughly assessed by using the results of each individual climate model (CGCM1, HadCM3, CSIRO9, HadRM2 and HIRHAM4) for climate change conditions to assess a parameter set for the random cascade precipitation model. These parameter sets have been used to generate for each climate model one realisation which served as input into the HBV-15 model. The results are given in Fig. 11,

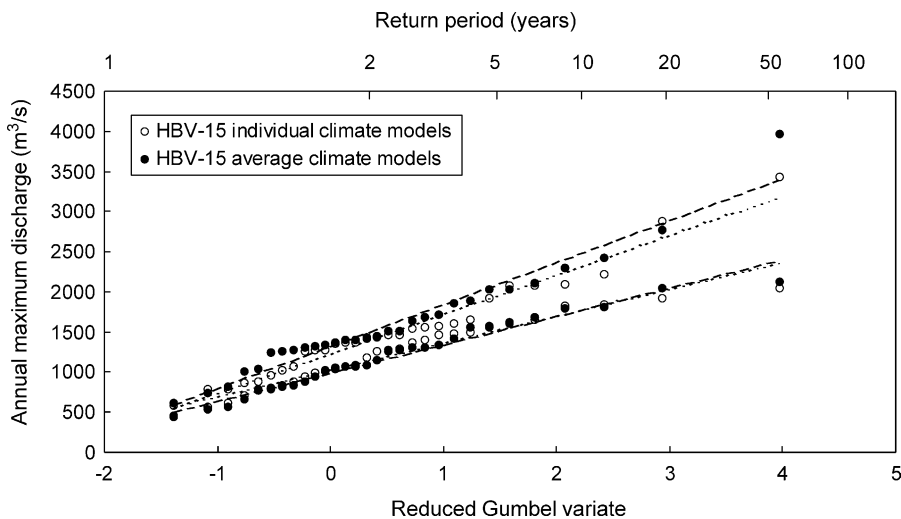


Fig. 11. Gumbel plot for annual maximum discharges for a 30-year period as simulated with five precipitation realisations derived from the average of the five climate models and five precipitation realisations derived from the five individual climate models under changed climate conditions for HBV-15. Only the minimum and maximum of each of the five realisations are shown. Regression lines for the 'realisations' (dashed) and realisations from 'individual climate models' (dotted) are given as well.

where the minimum and maximum of the five realisations of annual maximum discharges for a 30-year period are given. The results of Fig. 10 for HBV-15 under climate change conditions are shown as well for comparison. These results can be regarded as uncertainties in extreme discharges due to the stochasticity of the precipitation process. It is found in Fig. 11 that these uncertainties are even larger than the uncertainties in extreme discharges due to inter-model differences. The uncertainties due to individual climate model errors are unimportant here, because the climate model results have only been used to derive relative changes in observed precipitation statistics. It can be expected that the uncertainty in extreme discharges due to climate forcing uncertainties is at least as large as the two uncertainties in Fig. 11.

The differences between the results of HBV-1, HBV-15 and HBV-118 give some indication about uncertainties in extreme discharges due to uncertainties in model structure, although these differences are mainly scale related. Small differences between results of these different models have been found (5–10%) and therefore this uncertainty source seems to be relatively unimportant.

The effect of different key parameter values on the results was investigated in the calibration phase of the model, but mainly using HBV-1. In particular, variations of the parameters determining the fast runoff response (α and k_H) can have significant consequences for extreme discharges. For example, a 50% change of α results in approximately a 8% change in the 100-year return value. However, this reduction of uncertainty in parameters by the hydrological model (50–8%) is much larger than the reduction of uncertainty in precipitation statistics by the hydrological model (e.g. 15–6%), i.e. the model sensitivity to changes in parameters is much smaller than the sensitivity to changes in precipitation. The uncertainty in α and k_H is estimated at 20% resulting in a much smaller impact on the output uncertainty than for example the impact of precipitation uncertainty.

The uncertainty in extreme discharges due to extrapolation can be roughly assessed by using formulations, e.g. as proposed by Shaw (1983). The uncertainty in the estimation of the 100-year return value is 20% (one-sided) using a 90% confidence

interval and employing a 30-year series. The uncertainty is 25% when using a 95% confidence interval. This uncertainty can only be reduced by employing longer time series as can be done for the observed series (about 90 years, 12 and 15% uncertainty). This cannot be performed with respect to the modelled series for current and changed climate, because the hydrological model needs to be calibrated with a sufficient number of precipitation series of sufficient length. In this respect, the 30-year series currently is the maximum simulation length which can be used without arriving at a too coarse spatial precipitation scale. Other extreme value distributions (GEV, Pearson type-III) may slightly reduce uncertainties due to extrapolation.

Overall, the uncertainties in extreme discharges due to precipitation errors and extrapolation errors seem to be more important (more than 20 and about 20%, respectively) than uncertainties due to hydrological model errors and parameter estimation errors. These uncertainties should be quadratically summed, because of the general random character of the uncertainties resulting in an uncertainty of at least 30–40%.

6. Conclusions

An appropriate river basin model has been constructed by implementing the appropriate model components derived by Booij (2003) into the existing modelling framework HBV. Additionally, two other spatial resolutions for the hydrological model have been set up to evaluate the sensitivity of the model results to model resolution and to allow for a test of the model appropriateness procedure. The supposedly appropriate model has 118 sub-basins (HBV-118) and the additional models have 1 and 15 sub-basin(s) (HBV-1 and HBV-15). As far as possible, the three models were calibrated and validated with equal data series. Generations of a stochastic precipitation model under current and changed climate conditions have been used to assess the climate change impacts.

The average and extreme discharge behaviour at the basin outlet (Borgharen) is well reproduced by the three models in the calibration and validation, the results become somewhat better with increasing model resolution. The differences between

the average discharge behaviour of the sub-basins modelled by the two distributed models are small. Extreme discharges are generally better simulated by HBV-118 in the calibration, where in the validation HBV-15 is somewhat better. The model results with synthetic precipitation under current climate conditions show a small overestimation of average discharge behaviour and a considerable underestimation of extreme discharge behaviour. The underestimation of extreme discharges cannot be explained by the statistics of the synthetic precipitation input, but is caused by the observed precipitation input at the sub-basin scale. In most cases, this precipitation is not an areally averaged quantity, but rather a point quantity resulting in an overestimation of the standard deviation (variability) and extreme behaviour of observed precipitation at the sub-basin scale compared to the generated precipitation. This seems to be a very frequently occurring problem, which can be dealt with by increasing the density of precipitation stations in a river basin in an efficient manner.

The general trend with climate change is a small decrease of the average discharge and a small increase of the standard deviation of the discharge (variability) and extreme discharges. The range in extreme discharges for climate change conditions has increased with respect to the simulations for current climate conditions. This range results both from the stochasticity of the precipitation process and the differences between the climate models. Other uncertainties include those related to the river basin model structure, the parameter values and the extrapolation to large return periods. Overall, it appeared that the uncertainties in extreme discharges due to precipitation errors and extrapolation errors are more important than uncertainties due to hydrological model errors and parameter estimation errors. The total uncertainty is estimated at more than 40%. This problem of uncertainty associated with model outcomes is a phenomenon common to all scientific areas where approximations of reality by means of models are of interest. Numerous studies have assessed the different uncertainties (e.g. Uhlenbrook et al., 1999; Visser et al., 2000), but apparently no serious attempts have been made to evaluate the whole uncertainty cascade associated with the impact of climate change on river flooding. Given the complexity of in particular GCMs this seems to be very difficult if

not impossible to do, but at least some range of possible outcomes should accompany a climate impact study (e.g. Carter et al., 1999). Here, the uncertainty in river flooding with climate change (over 40%) is much larger than the change with respect to current climate conditions (less than 10%). However, climate changes are systematic changes rather than random changes and thus the uncertainty range will be shifted to another level corresponding to the changed average situation. Therefore, a certain confidence can be placed upon the direction of the change, provided that no ‘surprises’ such as the collapse of the thermohaline circulation in the North Atlantic (Ganopolski et al., 1998) or the disintegration of the West Antarctic Ice Sheet (Oppenheimer, 1998) will occur.

Acknowledgements

The daily station climatological data for Belgium and for France have been provided by respectively Luc Debontridder from the KMI (Belgian Royal Meteorological Institute) and Christophe Dehouck from Météo France. The daily HadCM3Gga1 and HadRM2 data have been kindly supplied by David Viner of the Climate Impacts LINK Project (DETR Contract EPG 1/1/68) on behalf of the Hadley Centre and U.K. Meteorological Office. The daily CGCM1 data have been acquired from the Canadian Centre for Climate Modelling and Analysis. The daily CSIRO9 data have been kindly provided by Janice Bathols of CSIRO Atmospheric Research. Ole Bøssing Christensen of the Climate Research Division of the Danish Climate Center prepared and helped a lot with the daily HIRHAM4 data. Bob Jones of the European Soil Bureau and Malene Bruun of the European Environmental Agency kindly supplied the soil and land use data, respectively. Eric Sprokkereef of RIZA gave the essential Meuse basin data and Joop Gerretsen of Rijkswaterstaat Limburg made the discharge data available. Sten Bergström of the Swedish Meteorological and Hydrological Institute kindly provided the HBV model. Koen van der Wal of the University of Twente contributed a lot by taking care of the HBV-118 simulations. The comments of Kees Vreugdenhil of the University of Twente and three

anonymous reviewers helped to improve the manuscript substantially.

References

- Abbott, M.B., Bathurst, J.C., Cunge, J.A., O'Connell, P.E., Rasmussen, J.L., 1986. An introduction to the European hydrological system—Système Hydrologique Europeen, SHE. 2. Structure of a physically-based, distributed modelling system. *J. Hydrol.* 87, 61–77.
- Bergström, S., 1990. Parameter values for the HBV model in Sweden (in Swedish). Technical Report no. 28, SMHI, Norrköping.
- Bergström, S., 1995. The HBV model. In: Singh, V.P. (Ed.), *Computer Models of Watershed Hydrology*. Water Resources Publications, Highlands Ranch, pp. 443–476.
- Bergström, S., Forsman, A., 1973. Development of a conceptual deterministic rainfall–runoff model. *Nord. Hydrol.* 4, 147–170.
- Bergström, S., Graham, L.P., 1998. On the scale problem in hydrological modelling. *J. Hydrol.* 211, 253–265.
- Beven, K., 1993. Prophecy, reality and uncertainty in distributed hydrological modelling. *Adv. Water Resour.* 16, 41–52.
- Beven, K.J., Calver, A., Morris, E.M., 1987. The Institute of Hydrology distributed model. Technical Report 98, Institute of Hydrology, Wallingford.
- Blöschl, G., Sivapalan, M., 1997. Process controls on regional flood frequency: coefficient of variation and basin scale. *Water Resour. Res.* 33, 2967–2980.
- Boer, G.J., Flato, G.M., Ramsden, D., 2000. A transient climate change simulation with greenhouse gas and aerosol forcing: projected climate to the twenty-first century. *Clim. Dynam.* 16, 427–450.
- Booij, M.J., 2002a. Appropriate modelling of climate change impacts on river flooding. PhD thesis, University of Twente, Enschede, ISBN: 90-365-1711-7.
- Booij, M.J., 2002b. Extreme daily precipitation in Western Europe with climate change at appropriate spatial scales. *Int. J. Climatol.* 22, 69–85.
- Booij, M.J., 2003. Determination and integration of appropriate spatial scales for river basin modelling. *Hydrol. Process.* 17, 2581–2598.
- Bossard, M., Steenmans, Ch., Feranec, J., Otahel, J., 2000. The revised and supplemented Corine land cover nomenclature. Technical Report 38, European Environment Agency, Copenhagen.
- Brandsma, Th., 1995. Hydrological impact of climate change: a sensitivity study for the Netherlands. PhD thesis, Delft University of Technology, Delft.
- Burnash, R.J.C., 1995. The NWS river forecast system—catchment modeling. In: Singh, V.P. (Ed.), *Computer Models of Watershed Hydrology*. Water Resources Publications, Highlands Ranch, pp. 311–366.
- Carter, T.R., Hulme, M., Lal, M., 1999. Guidelines on the use of scenario data for climate impact and adaptation assessment. Version 1, Technical Report, IPCC-TGCI, Norwich.
- Christensen, J.H., Christensen, O.B., Lopez, P., Meijgaard, E., van and Botzet, M., 1996. The HIRHAM4 regional atmospheric climate model. Scientific Report 96-4, Danish Meteorological Institute, Copenhagen.
- Crawford, N.H., Linsley, R.K., 1966. Digital simulation in hydrology—Stanford watershed model IV. Technical Report 39, Stanford University, Stanford.
- Diermanse, F.L.M., 2001. Physically based modelling of rainfall–runoff processes. PhD thesis, Delft University Press, Delft.
- Feldman, A.D., 1995. HEC-1 flood hydrograph package. In: Singh, V.P. (Ed.), *Computer Models of Watershed Hydrology*. Water Resources Publications, Highlands Ranch, pp. 119–150.
- Franchini, M., Pacciani, M., 1991. Comparative analysis of several conceptual rainfall–runoff models. *J. Hydrol.* 122, 161–219.
- Ganopolski, A., Rahmstorf, S., Petoukhov, V., Claussen, M., 1998. Simulation of modern and glacial climates with a coupled global model of intermediate complexity. *Nature* 391, 351–356.
- Gellens, D., Roulin, E., 1998. Streamflow response of Belgian catchments to IPCC climate change scenarios. *J. Hydrol.* 210, 242–258.
- Goel, N.K., Kurothe, R.S., Mathur, B.S., Vogel, R.M., 2000. A derived flood frequency distribution for correlated rainfall intensity and duration. *J. Hydrol.* 228, 56–67.
- Gordon, H.B., O'Farrell, S.P., 1997. Transient climate change in the CSIRO coupled model with dynamic sea ice. *Mon. Weather Rev.* 125, 875–907.
- Gordon, C., Cooper, C., Senior, C., Banks, H., Gregory, J., Johns, T., Mitchell, J., Wood, R., 2000. The simulation of SST, sea ice extents and ocean heat transports in a version of the Hadley Centre coupled model without flux adjustments. *Clim. Dynam.* 16, 147–168.
- Harlin, J., Kung, C.-S., 1992. Parameter uncertainty and simulation of design floods in Sweden. *J. Hydrol.* 137, 209–230.
- Huber, W.C., 1995. EPA storm water management model—SWMM. In: Singh, V.P. (Ed.), *Computer Models of Watershed Hydrology*. Water Resources Publications, Highlands Ranch, pp. 783–808.
- IPCC, 2001. Climate change 2001: the scientific basis. In: Houghton, J.T., Ding, Y., Griggs, D.J., Noguer, M., van der Linden, P.J., Dai, X., Maskell, K. (Eds.), *Contribution of Working Group I to the Third Assessment Report of the Intergovernmental Panel on Climate Change*. Cambridge University Press, Cambridge.
- Jacobs, P., Blom, G., Linden, G. van der, 2000. Climatological changes in storm surges and river discharges: the impact on flood protection and salt intrusion in the Rhine-Meuse delta. Proceedings of the ECLAT-2 KNMI Workshop. Climatic Research Unit, Norwich, pp. 35–48.
- Jones, R.G., Murphy, J.M., Noguer, M., 1995. Simulation of climate change over Europe using a nested regional-climate model. I. Assessment of control climate, including sensitivity to location of lateral boundaries. *Q. J. R. Meteor. Soc.* 121, 1413–1449.
- Killingtveit, A., Sælthun, N.R., 1995. Hydropower development: hydrology. Technical Report, Norwegian Institute of Technology, Oslo.

- King, D., Daroussin, J., Tavernier, R., 1994. Development of a soil geographical database from the soil map of the European Communities. *Catena* 21, 37–56.
- Kite, G.W., 1995. The SLURP model. In: Singh, V.P. (Ed.), *Computer Models of Watershed Hydrology*. Water Resources Publications, Highlands Ranch, pp. 521–562.
- Kite, G.W., Kouwen, N., 1992. Watershed modeling using land classifications. *Water Resour. Res.* 28, 3193–3200.
- Krysanova, V., Bronstert, A., Müller-Wohlfeil, D.-I., 1999. Modelling river discharge for large drainage basins: from lumped to distributed approach. *Hydrol. Sci. J.* 44, 313–331.
- Lamb, R., 1999. Calibration of a conceptual rainfall–runoff model for flood frequency estimation by continuous simulation. *Water Resour. Res.* 35, 3103–3114.
- Leavesley, G.H., Lichty, R.W., Troutman, B.M., Saindon, L.G., 1983. Precipitation-runoff modeling system. User manual. USGS water resources investigations report 83-4238, USGS, Denver.
- Lindström, G., Johansson, B., Persson, M., Gardelin, M., Bergström, S., 1997. Development and test of the distributed HBV-96 hydrological model. *J. Hydrol.* 201, 272–288.
- Middelkoop, H., Parmet, B., 1998. Assessment of the impact of climate change on peak flows in the Netherlands—a matter of scale. *Proceedings of the Second International Conference on Climate and Water*, Helsinki University of Technology, Helsinki, pp. 20–33.
- Nash, J.E., Sutcliffe, J.V., 1970. River flow forecasting through conceptual models. Part I—a discussion of principles. *J. Hydrol.* 10, 282–290.
- Oppenheimer, M., 1998. Global warming and the stability of the West Antarctic Ice Sheet. *Nature* 393, 325–332.
- Over, T.M., Gupta, V.K., 1996. A space–time theory of mesoscale rainfall using random cascades. *J. Geophys. Res.* 101, 26319–26331.
- Passchier, R.H., 1996. Evaluation hydrologic model packages. Technical Report Q2044, WL/Delft Hydraulics, Delft (www.wldelft.nl).
- Rawls, W.J., Ahuja, L.R., Brakensiek, D.L., Shirmohammadi, A., 1993. Infiltration and soil water movement. In: Maidment, D.R. (Ed.), *Handbook of Hydrology*. McGraw-Hill, New York (Chapter 5).
- Refsgaard, J.C., 1996. Terminology, modelling protocol and classification of hydrological models. In: Abbott, M.B., Refsgaard, J.C. (Eds.), *Distributed Hydrological Modelling*. Kluwer, Dordrecht, pp. 17–39.
- RIZA, 2000. Topographic data for the Meuse basin. Technical Report, RIZA, Arnhem.
- Seibert, J., 1999. Regionalisation of parameters for a conceptual rainfall–runoff model. *Agric. Forest Meteorol.* 98, 279–293.
- Shaw, E.M., 1983. *Hydrology in Practice*. Chapman & Hall, London.
- SMHI, 1999. *Integrated Hydrological Modelling System (IHMS)*. Manual version 4.3. SMHI, Norrköping.
- Uhlenbrook, S., Seibert, J., Leibundgut, C., Rodhe, A., 1999. Prediction uncertainty of conceptual rainfall–runoff models caused by problems in identifying model parameters and structure. *Hydrol. Sci. J.* 44, 779–797.
- US Geological Survey, 1996. Global 30-arc second elevation data set. Technical Report, USGS, Sioux Falls.
- Van der Wal, K.U., 2001. Meuse model moulding. On the effect of spatial resolution. MSc thesis, University of Twente, Enschede.
- Visser, H., Folkert, R.J.M., Hoekstra, J., de Wolff, J.J., 2000. Identifying key sources of uncertainty in climate change projections. *Clim. Change* 45, 421–457.
- Wilks, D.S., 1998. Multisite generalization of a daily stochastic precipitation generation model. *J. Hydrol.* 210, 178–191.
- Ye, W., Bates, B.C., Viney, N.R., Sivapalan, M., Jakeman, A.J., 1997. Performance of conceptual rainfall–runoff models in low-yielding ephemeral catchments. *Water Resour. Res.* 33, 153–166.